



1 Recovery of Strength in Thermally Cracked Freshwater and Salt- 2 Water Ice

3 Andrii Murdza¹, Erland M. Schulson¹, Carl E. Renshaw^{1,2}

4 ¹ Thayer School of Engineering, Dartmouth College, Hanover, NH (USA).

5 ² Department of Earth Sciences, Dartmouth College, Hanover, NH (USA).

6 *Correspondence to:* Andrii Murdza (Andrii.Murdza@Dartmouth.edu)

7 **Abstract.** The integrity of ocean and lake ice covers is increasingly threatened by climate change, which reduces ice
8 extent and promotes breakup. In addition to thinner ice and larger waves, thermal cracking may also contribute to
9 ice cover failure. This study investigates the impact of thermal cracking on the flexural strength of freshwater and
10 sea ice. Laboratory experiments show that when a narrow region of ice is thermally shocked, the flexural strength of
11 both freshwater and sea ice initially decreases but subsequently recovers completely. In contrast, when the entire
12 surface is thermally shocked, strength recovery is only partial in freshwater ice, while sea ice again fully recovers its
13 strength. Repeated cycles of cracking followed by healing do not affect the recovered flexural strength. Additional
14 experiments involving creep demonstrate that compressive stress enhances healing, highlighting the role of ice
15 sintering in strength recovery. The differing behavior between localized and full-surface cracking is attributed to
16 residual compressive stresses that develop during healing when only a narrow region is shocked. Rapid healing
17 observed in sea ice is likely facilitated by its porous structure and the presence of brine, suggesting that natural sea
18 ice may retain significant mechanical integrity even after thermal cracking.

19 1 Introduction

20 The structural integrity of ocean and lake ice covers faces a growing threat (Filazzola et al., 2024; King et al., 2026;
21 Kwok and Rothrock, 2009; Stroeve et al., 2011). Understanding the mechanical characteristics of ice covers, for
22 example in the Great Lakes, is essential for ensuring the safety and design of infrastructure (Bruce Martin and Cott,
23 2016; Millerd, 2011; Timco and Weeks, 2010). The ongoing reduction in ice cover extent due to climate change
24 (e.g., NSIDC, 2022), coupled with the simultaneous factors of thinner ice and the presence of larger waves due to
25 increased fetch (Li and Du, 2016; Thomson et al., 2018), makes the remaining ice cover more susceptible to
26 fragmentation. The potential consequences of this situation are negatively affecting wave attenuation (Squire, 2007),
27 coastal erosion (Jones et al., 2009; Overeem et al., 2011), shipping (Stewart et al., 2007), albedo (Perovich et al.,
28 2001; Pistone et al., 2014; Zhang et al., 2019), and rate of ice melting (Rampal et al., 2009). One of the processes
29 that could contribute to ice cover breakup is thermal cracking which generates defects of varying lengths, from
30 submeter to several kilometers (Evans and Untersteiner, 1971). The cracks concentrate stress that originates from
31 deformation induced by wind and ocean currents. This stress concentration from smaller cracks can lead to the
32 development of large-scale cracks (Schulson and Duval, 2009) that imperil the integrity of the cover.



33 The issue of thermal cracks in ice has been addressed in previous studies (Barrette and Charlebois, 2018; Barrette
34 and Jordaan, 2002; Bazant, 1992; Colbeck, 1986; Fisher, 2005; Fransson, 1991; Gold, 1961, 1963; Milne, 1972;
35 Yang et al., 2018). However, to the best of our knowledge, there has been no comprehensive study exploring the
36 long-term impact of thermal cracks on ice strength and their influence on ice behavior under dynamic loading.

37 To obtain some insight into how thermal cracks impact structural integrity, we recently conducted a preliminary
38 study to investigate how thermal cracks affect flexural strength of both sea ice and freshwater ice at temperatures
39 from -78°C to -3°C (Murdza et al., 2022a). In that study, small beams of ice were thermally shocked by spraying
40 liquid nitrogen across a narrow band in the middle of one of their largest faces. Afterwards, the cracked ice was bent
41 to failure under four-point loading, ensuring that the cracked surface experienced tensile stresses. The cracks
42 initially weakened the materials, in accord with the dictates of fracture mechanics, but not for long. Within a short
43 period of time, typically of the order of minutes, the flexural strength recovered completely: the cracks had healed.
44 In most instances, after the ice had healed, terminal fracture occurred outside the area of remnant scars that marked
45 the pre-cracked region, suggesting that the healed region may have been as strong as or stronger than the
46 surrounding pristine ice. If thermal cracks heal rapidly, their long-term impact on the mechanical integrity of ice
47 covers may be significantly smaller than previously assumed.

48 A limitation of the previous investigation (Murdza et al., 2022a) was its focus on cracking a narrow band on the ice
49 surface – a scenario less common in real-world applications. Here we consider the more common scenario where
50 the entire surface of the ice is thermally cracked. Specifically, the present study aims to explore how thermal shock
51 and subsequent healing impact the flexural strength of both freshwater ice and sea ice. Applying thermal shock to a
52 larger area provides more relevant insights for situations where cracking occurs due to rapid air temperature
53 fluctuations. It is relevant not only to fractures occurring in sea ice but also to any ice cover, terrestrial or
54 extraterrestrial (Goldreich and Mitchell, 2010; Hirata et al., 2022).

55 In addition, this study explores several related aspects of the healing process, including whether healing can restore
56 or even enhance the strength of previously cracked regions relative to pristine ice, whether repeated cycles of
57 cracking and healing lead to cumulative strengthening, and the role of contact stresses at points of contact
58 (asperities) during thermal expansion in promoting healing.

59 To address these questions, we conducted a new series of experiments where we sprayed with liquid nitrogen the
60 whole sample surface, instead of a narrow band only. We conducted these experiments on both freshwater ice and
61 first-year sea ice. In addition, to further investigate the role of pressure on the healing process we conducted creep
62 experiments on thermally shocked ice. In the sections to follow, we describe our observations and discuss the
63 processes responsible for strength recovery.

64 As will become apparent, the results indicate that strength recovery in thermally cracked ice may occur through two
65 distinct processes. First, healing may occur when opposing crack surfaces come into contact, allowing sintering
66 across the crack interface; the presence of a liquid-like layer at crack surfaces may further facilitate this process,

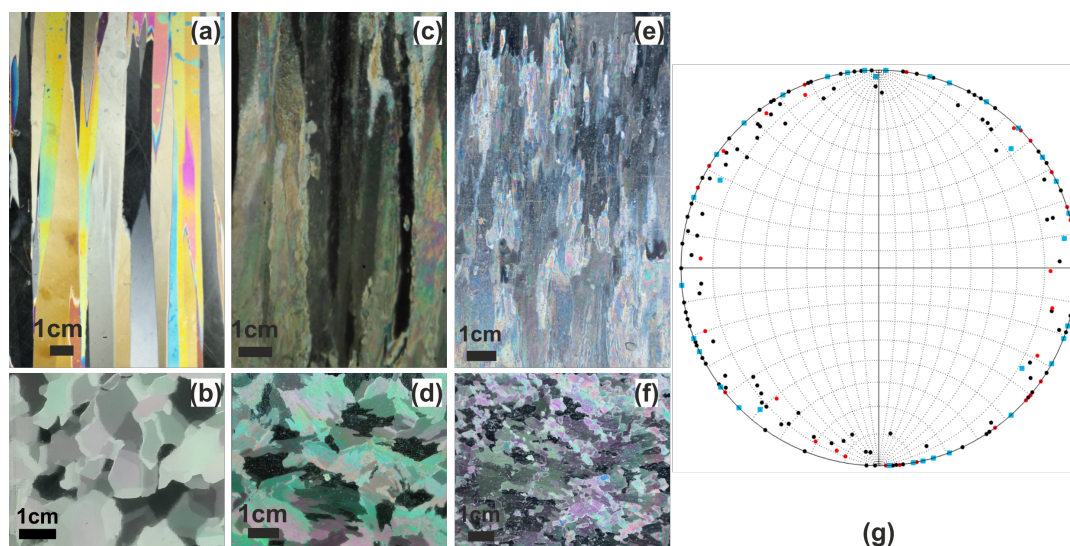


67 particularly in sea ice where brine and porosity enhance mass transport. Second, even when crack surfaces remain
68 separated and cannot sinter, strength recovery may occur through creep-assisted blunting of crack tips. The relative
69 importance of these processes depends on temperature and loading conditions.

70 **2 Materials and Methods**

71 We studied the behavior of three types of ice: S2 laboratory-grown freshwater ice (i.e., salt-free), laboratory-grown
72 saline ice and first-year sea ice, as previously investigated (Murdza et al., 2020, 2021c, 2022a, 2023; Schulson et al.,
73 2022). The freshwater and saline ice were produced in the laboratory through a standard procedure, involving the
74 unidirectional solidification of either local tap water (Golding et al., 2014; Smith and Schulson, 1993) or local tap
75 water that had been salted with the commercial product “Instant Ocean” to a salinity of 17.5 parts per thousand
76 (Golding et al., 2014). The sea ice was collected as submeter-sized blocks from the Beaufort Sea's ice cover during
77 the winter of 2020 and stored at -30°C in Dartmouth's Ice Research Laboratory. All types of ice were polycrystalline
78 aggregates, characterized by columnar-shaped grains oriented with their long axes parallel to the growth direction,
79 Fig. 1. They exhibited the S2 crystallographic growth texture, with grain c-axes primarily within the horizontal plane
80 but oriented randomly within that plane. The grain size (column diameter) of the freshwater ice was 5.5 ± 1.3 mm,
81 with a density of 914.1 ± 1.6 $\text{kg}\cdot\text{m}^{-3}$. The laboratory-grown saline ice had a grain size of 3.8 ± 0.9 mm, with a
82 density of 878 ± 11 $\text{kg}\cdot\text{m}^{-3}$ and a salinity of 3.0 ± 0.9 ppt. The first-year sea ice had a grain size of 2.7 ± 0.4 mm, a
83 density of 906 ± 4 $\text{kg}\cdot\text{m}^{-3}$, and a salinity of 3.0 ± 0.3 ppt.

84 Grain size was measured manually from horizontal thin sections prepared from tested ice beams. For each thin
85 section, five horizontal and five vertical lines were drawn and the mean grain diameter was estimated using the
86 linear intercept method by dividing the total line length by the number of grain boundaries intersected by the line.
87 Approximately 500 grains were measured for each ice type. Density was determined from rectangular prism-shaped
88 specimens cut and milled from tested ice beams. The dimensions of each specimen were measured using calipers
89 and the mass was measured using a digital balance. The density was then calculated from the measured mass and
90 volume. To improve accuracy, relatively large specimens were used whenever possible. Reported uncertainties in
91 density represent propagated measurement uncertainty based on repeated measurements of mass and dimensions.
92 Salinity of saline and sea ice was measured by melting individual samples and measuring the salinity of the
93 meltwater using a digital conductivity meter. Reported salinity uncertainties represent standard deviations from
94 measurements of multiple samples.



95

96 **Figure 1. Photomicrographs of ice microstructure: vertical (a) and horizontal (b) thin sections of freshwater ice, vertical**
 97 **(c) and horizontal (d) thin sections of saline ice, vertical (e) and horizontal (f) thin sections of sea ice, and stereographic**
 98 **projection plot of crystal c-axis {0001} orientations freshwater (in black), saline (in red) and sea ice (in blue) (g).**
 99

100 From these materials, test specimens were machined and milled into thin beams with final dimensions: thickness $h =$
 101 13 mm (along the columns), width $w = 75$ mm, and length $l = 300$ mm. To explore the effect of temperature on
 102 kinetics and hence to gain some insight into the physical mechanism underlying healing, the specimens were tested at
 103 either -78 °C, -28 °C, -10 °C or -3 °C. Each specimen was oriented such that its long axis was perpendicular to the
 104 direction of loading upon bending, ensuring that the ice was loaded across the columnar-shaped grains, analogous to
 105 the natural loading of an ice cover (Iliescu et al., 2017; Murdza et al., 2021a, b, 2022b). After achieving thermal
 106 equilibrium, the beams were subjected to thermal shock by briefly spraying them with liquid nitrogen, either across
 107 a narrow (~ 20 mm) band in the middle of one of the largest faces or across the complete surface of one of the
 108 largest faces. The thermal shock created a network of randomly oriented, grain-sized thermal cracks, both
 109 intergranular and transgranular, that partially penetrated the beam to about one-fourth to one-third of its thickness, as
 110 in the previous studies (Murdza et al., 2022a, 2023). The cracks in the sea ice vanished rapidly, typically within less
 111 than 10 seconds, at least as far as the naked eye could discern. For ease of reference to our earlier work, Fig. 1 in
 112 Murdza et al. (2022a) shows cracks in the salt-free ice and the video in supporting information of that reference
 113 shows them in the sea ice where they vanished quickly.
 114

115 The present manuscript combines newly acquired experimental results with selected previously published datasets
 116 (Murdza et al., 2022a, 2023) to investigate and understand the processes responsible for healing in thermally cracked
 117 ice. The narrow-band thermal cracking experiments are summarized from Murdza et al. (2022a) for comparison
 118 (number ii below), whereas the full-surface thermal cracking, repeated cracking–healing, compressive-creep, and
 119 sea-ice cyclic-loading experiments are newly reported here. Some cyclic-loading results from Murdza et al. (2023)
 120 are also reinterpreted in the context of creep-assisted crack-tip blunting. The experimental sets are described below.

- 121 (i) *Healing after full-surface thermal cracking.* Some freshwater and sea ice beams were subjected to
 122 thermal shock, ensuring complete coverage of one of the largest faces of the sample, which
 123 induced cracking of the whole surface. The experiments were performed at -10 °C. The cracked
 124 specimens were allowed to heal for a period of up to 12 hours by placing them in sealed plastic



125 bags inside a foam box in a cold room at the same temperature of $-10\text{ }^{\circ}\text{C}$. Afterward, the cracked
126 beams were placed in a 4-point loading frame and then bent to failure such that the cracked
127 surface was loaded in tension.
128
129 (ii) *Healing after narrow-band thermal cracking.* Some freshwater, saline and sea ice beams were
130 thermally shocked across a narrow ($\sim 20\text{ mm}$) band and then subjected to failure under 4-point
131 loading, after varying the time elapsed between shocking and bending from 0 to ~ 20 hrs. These
132 experiments were conducted at temperatures of $-78\text{ }^{\circ}\text{C}$, $-28\text{ }^{\circ}\text{C}$, $-10\text{ }^{\circ}\text{C}$ or $-3\text{ }^{\circ}\text{C}$.
133
134 (iii) *Repeated cycles of cracking and healing.* Some of the freshwater ice beams underwent a process
135 involving five cycles of cracking of the entire surface followed by subsequent healing before they
136 were subjected to bending. In these tests, the intervals of healing between thermal shocks ranged
137 from 1 hour to 3 days, with the same interval applied consistently throughout all five cracking-
138 cum-healing cycles for each specific sample. For instance, a five-cycle test with healing intervals
139 of 3 days was performed over a period of 15 days. These experiments were performed at $-10\text{ }^{\circ}\text{C}$.
140
141 (iv) *Effect of compressive stresses on healing.* Some freshwater ice beams were subjected to full-
142 surface thermal shocking and then immediately after shocking were subjected for 1 hour to a creep
143 load that generated an outer-fiber compressive stress on the cracked surface of 1 MPa.
144 Subsequently, the samples were bent to failure with the cracked surface under tension. These
145 experiments were performed at $-10\text{ }^{\circ}\text{C}$.
146
147 (v) *Creep-assisted crack-tip blunting.* To investigate the effect of thermal shock and creep assisted
148 crack-tip blunting on the behavior of freshwater ice under non-reversed cyclic flexing, we
149 introduced the thermal shock during the first cycle to a narrow ($\sim 20\text{ mm}$) band. Cycling of cracked
150 specimens was done by flexing under 4-point loading at either $-10\text{ }^{\circ}\text{C}$ or $-28\text{ }^{\circ}\text{C}$. In order to
151 eliminate the potential for opposing crack surfaces to come into contact, we cycled specimens in a
152 non-reversed manner such that the shocked region was always under tension. In these
153 experiments, the minimum outer-fiber stress, defined below, was either 0.3 or 0.5 MPa, while the
154 maximum outer-fiber stress was initially 0.6 MPa and then was gradually increased up to 1.1 MPa
155 to reach higher outer-fiber stress amplitudes during cycling, in the manner described earlier
156 (Murdza et al., 2020). Eventually, samples were cycled in tension between either 0.3 MPa and
157 1.1 MPa or 0.5 MPa and 1.1 MPa for an additional number of cycles ranging from 50 to $\sim 20,000$,
158 and then monotonically brought to failure, again, such that the cracked surface was under tension.
159 In this case, stress amplitude, which is defined as one-half of the difference between the maximum
160 and the minimum outer-fiber stress, was either 0.4 or 0.3 MPa, while the mean stress, which is
161 defined as one-half the sum of the maximum stress and the minimum stress, was either 0.9 or
162 0.8 MPa, respectfully. In a few experiments, instead of cycling, we crept the sample at 0.8 MPa
163 for $\sim 10,000$ sec.
164 Similar experiments on crack-assisted blunting were also performed on first-year sea ice at
165 $-10\text{ }^{\circ}\text{C}$. In these tests the specimens were cycled between outer-fiber tensile stresses of 0.5 and 0.7
166 MPa for either 10,000 or 20,000 cycles, with thermal shock applied to the surface that would
167 subsequently experience tensile stress.

168

169 During both bending and cycling, the samples were loaded across the columns at a constant outer-fiber center-point
170 strain rate of $\sim 10^{-4}\text{ s}^{-1}$, always taking care to ensure that the cracked face was under tension (Murdza et al., 2023).
171 The flexural strength σ_f was obtained from the load at failure, P , using the four-point loading relationship:



172

$$\sigma_f = \frac{3PL}{4bh^2}, \quad (1)$$

173

174 where $L = 254$ mm is the distance between the outer pair of load lines and b and h denote the width and thickness of
175 the beam, respectively.

176 3 Results

177 Including our earlier experiments (Murdza et al., 2022a) a total of 213 flexural strength measurements were made
178 across all experimental conditions. Fewer tests were conducted on sea ice owing to the limited availability of the
179 material. Results for each experiment are available in the data repository. The results are categorized based on the
180 types of experiments as outlined in the previous section.

181 (i) *Healing after full-surface thermal cracking.* After thermally cracking the whole surface,
182 freshwater samples underwent a single 12-hour healing period, while sea ice samples were
183 allowed to heal for 1 hour. Subsequently, the flexural strength of the healed freshwater ice was 1.3
184 ± 0.1 MPa; similarly, the strength of the sea ice was 1.3 ± 0.3 MPa. For reference, the strength of
185 the as-cracked ice (i.e., zero elapsed time since thermal cracking) was ~ 0.7 MPa for both the salty
186 and the salt-free materials (Murdza et al., 2022), in keeping with the dictates of fracture
187 mechanics; the strength of pristine, non-cracked freshwater and sea ice was 1.67 ± 0.22 MPa and
188 1.40 ± 0.07 MPa, respectively. In other words, both materials recovered to nearly twice their as-
189 cracked strength, which for sea ice was comparable to the strength of intact sea ice.

190
191 (ii) *Healing after narrow-band thermal cracking.* Figure 2 illustrates the effect of the elapsed time on
192 flexural strength. These results are discussed in detail in Murdza et. al. (2022). In brief, for each
193 material and at each of the three temperatures explored, immediately after the thermal shock the
194 flexural strength of ice was significantly reduced in accord with fracture mechanics, but then
195 rapidly recovered completely and reached the strength of non-cracked ice. At the same
196 temperature, the healing time was greater in the freshwater ice than in the sea ice.

197
198 (iii) *Repeated cycles of cracking and healing.* Following five cycles of thermal cracking of the entire
199 surface and subsequent healing of freshwater ice, the flexural strength was measured as $1.28 \pm$
200 0.08 MPa. This value is comparable to the strength obtained after a single cracking–healing event
201 (1.3 ± 0.1 MPa), indicating that repeated cycles of cracking and healing do not lead to further
202 strengthening of the material.

203 In one additional experiment, after completing five cracking–healing cycles with healing intervals



204 of 3 days, a specimen was subjected to bending while thermal shock was applied simultaneously.
205 In this case, failure occurred at 0.56 MPa, a value consistent with the strength of ice that is
206 thermally cracked and loaded immediately after shocking. This observation further indicates that
207 repeated cracking-cum-healing *does* not increase the inherent resistance of the material to thermal
208 cracking.

209
210 (iv) *Effect of compressive stresses on healing.* In this set of experiments where the thermally cracked
211 surface of freshwater ice was crept under compression before being bent to failure under tension,
212 the measurements yielded a flexural strength of 1.56 ± 0.13 MPa. This value approaches the
213 strength of pristine freshwater ice (1.67 ± 0.22 MPa), indicating that compressive stress during
214 healing significantly enhances strength recovery.

215
216 (v) *Creep-assisted crack-tip blunting.* Figure 3 shows the effect of cycling on the recovery of strength.
217 At -10 °C, the strength of freshwater ice recovered completely after $\sim 10,000$ cycles, approaching
218 the strength of pristine ice, whereas at -28 °C recovery remained incomplete even after $\sim 20,000$
219 cycles, with the strength reaching only 1.23 ± 0.12 MPa. Similarly, following approximately 10
220 hours of creep at 0.8 MPa (equivalent to the duration of the cycling experiments) at -10 °C, the
221 flexural strength of the freshwater ice also exhibited complete recovery. Several freshwater
222 specimens failed during the early stages of cycling at -10 °C while being loaded (Fig. 3),
223 indicating relatively low strength prior to full recovery.
224 In similar experiments on first-year sea ice conducted at -10 °C, the strength recovered
225 completely after $\sim 10,000$ cycles, reaching 1.32 ± 0.22 MPa, which is comparable to the strength of
226 pristine sea ice (1.40 ± 0.07 MPa).

227 To demonstrate that the observed recovery of strength in freshwater ice cannot be explained solely by the warming
228 of the thermally shocked beam, we compared the time scales of temperature recovery and strength recovery, finding
229 that the surface temperature recovers much more rapidly than the strength. Figure 2 shows the effect of elapsed time
230 on flexural strength of freshwater ice and salt-water ice at different temperatures (Murdza et al., 2022a). The
231 recovered strength was normalized by dividing by the maximum strength recovery

$$\frac{\sigma - \sigma_{t=0}}{\sigma_0 - \sigma_{t=0}}, \quad (2)$$

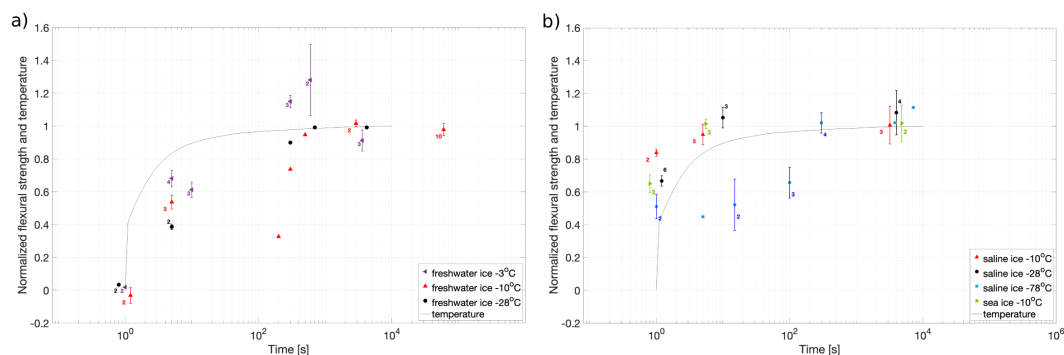
232 where $\sigma_{t=0}$ is strength of ice immediately after thermal shock, σ_0 is strength of pristine non-cracked ice). This figure
233 additionally illustrates the normalized ice surface temperature change of the thermally shocked surface immediately
234 following the shock



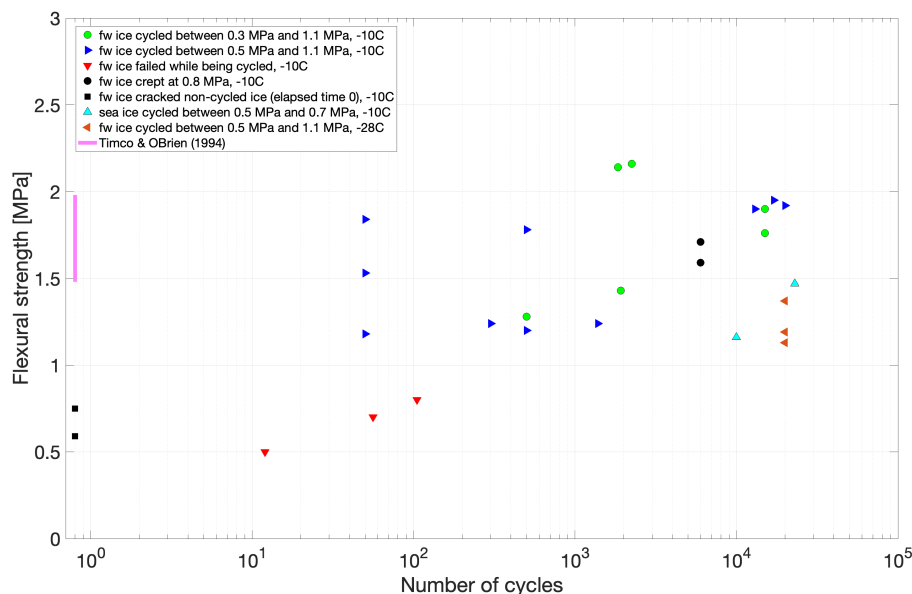
$$\frac{T(t) - T_N}{T_o - T_N} \tag{3}$$

235 where $T(t)$ is the surface temperature of the ice as a function of time t , T_N is the temperature of the liquid nitrogen (-
 236 196°C), and T_o is the temperature of the cold room (see Supporting Information). It is worth noting that in
 237 freshwater ice the surface temperature recovers significantly faster than strength; the majority of the temperature
 238 recovery takes place within the initial 4 seconds (from -196°C to -40°C), whereas strength predominantly recovers
 239 over approximately 100-300 seconds. In contrast, in salt-water ice the recovery time of strength is comparable to the
 240 time scale of temperature recovery, suggesting that the mechanisms governing healing in saline ice may differ from
 241 those in freshwater ice.

242 Taken together, these results demonstrate that thermally induced cracks in ice can heal through multiple processes,
 243 and that the rate and extent of strength recovery depend on temperature, loading conditions and the geometry of the
 244 cracked region.



245
 246 **Figure 2. Flexural strength recovery of cracked and healed freshwater ice (a) and salt-water ice (b), normalized by the**
 247 **maximum strength recovery, plotted against time since thermal cracking at various temperatures. Error bars indicate**
 248 **standard errors with the number of samples indicated by the number next to the point. The solid line illustrates the**
 249 **normalized surface temperature at the center of the beam, with respect to the temperature of the cold room. Modified**
 250 **after (Murdza et al., 2022a).**



251

252 **Figure 3. Flexural strength of cracked freshwater ice at -10°C as a function of number of cycles during non-reversed**
 253 **cycling. The solid pink line indicates the average flexural strength of non-cracked non-cycled freshwater ice plus and**
 254 **minus one standard deviation, that is, 1.73 ± 0.25 MPa (Timco and O'Brien, 1994).**

255

256 **4 Discussion**

257 The primary objective of the present study was to investigate the effect of thermal shock on the flexural strength of
 258 both freshwater ice and sea ice and to identify the processes responsible for strength recovery. Based on the
 259 experimental observations, we propose that strength recovery occurs through two primary processes. The first
 260 involves healing through contact between opposing crack surfaces, where sintering via surface diffusion and the
 261 presence of a liquid-like layer promote the formation of bonds across the crack interface (Nguyen et al., 2021). This
 262 process can be significantly enhanced when compressive stresses increase the real area of contact between crack
 263 faces. The second process involves creep-assisted blunting of crack tips, a thermally activated mechanism that
 264 reduces stress concentration and allows recovery of strength even when crack surfaces remain separated. The
 265 relative importance of these processes depends on temperature, loading conditions and whether opposing crack
 266 surfaces are able to come into contact.

267 When the entire surface of a freshwater ice sample is subjected to thermal cracking, the initial flexural strength
 268 decreases to approximately 0.7 MPa, consistent with the expectations of fracture mechanics (see analysis in Murdza
 269 et al., 2022a). After a healing period of approximately 12 hours, the strength recovers to approximately 1.3 MPa. In
 270 these experiments, terminal fractures always propagated along at least one of the original thermal cracks, suggesting
 271 that the healed cracks still represented relatively weak regions within the ice structure. We therefore attribute the



272 observed partial strength recovery to healing processes occurring at the crack surfaces, primarily through the
273 combination of sintering and of the transformation of the liquid-like layer (Asakawa et al., 2016; Dash et al., 1995;
274 Elbaum and Schick, 1991; Faraday, 1860; Petrenko and Whitworth, 1999; Szabo and Schneebeli, 2007) into solid
275 ice.

276 Experiments involving repeated cycles of cracking of the entire surface followed by healing indicate that this
277 process restores strength but does not lead to progressive strengthening of the material. After several cracking–
278 healing cycles, the measured flexural strength remained comparable to that of specimens that experienced a single
279 cracking event, suggesting that the healing mechanisms primarily restore the original strength rather than enhance it.

280 A different behavior is observed when only a narrow band of the ice surface is thermally shocked. In this case,
281 although the initial strength again decreases to approximately 0.7 MPa, the flexural strength recovers completely
282 within a relatively short period of approximately 300 s (Murdza et al., 2022a). The faster and more complete
283 recovery is likely due to the presence of compressive stresses generated during the warming of the thermally
284 shocked region. Immediately following thermal shock, the surface layer contracts due to rapid cooling and cracks
285 form. As the shocked region subsequently warms, thermal expansion occurs while the surrounding material
286 constrains this expansion. This constraint generates compressive stresses within the cracked region. These stresses
287 increase the real area of contact between opposing crack faces and promote healing through creep and sintering
288 (Schulson et al., 2016; Schulson and Fortt, 2013).

289 Consistent with this interpretation, in the majority of narrow-band experiments (22 out of 25 tests) the final fracture
290 after healing propagated outside the thermally shocked region (Murdza et al., 2022a). This observation suggests that
291 the healed region may be as strong as, or even stronger than, the surrounding pristine ice. One possible explanation
292 is that the compressive stresses and creep deformation occurring during healing lead to plastic deformation along the
293 crack surfaces and to potentially dynamic recrystallization, resulting in locally finer grain sizes. Since the tensile
294 strength of ice is known to increase with decreasing grain size (Schulson and Duval, 2009), this microstructural
295 change could locally enhance strength. Whether such recrystallization actually occurred remains to be determined.
296 However, an alternative explanation is also possible. If the healed region has the same strength as the surrounding
297 material, fractures may occur more frequently outside the shocked region simply because the cracked region
298 occupies a smaller area within the beam section between the loading spans. Therefore, statistically, fractures are
299 more likely to happen in the larger area.

300 When the entire surface of the ice specimen is thermally shocked, the situation differs because the shocked region is
301 not confined by surrounding non-cracked material during subsequent warming (although there may still be some
302 internal pressure as the ice warms up). As a result, the generation of compressive stresses is significantly reduced.
303 The absence of substantial confinement limits the extent to which opposing crack faces are forced into contact, and
304 consequently the ability of the material to regain strength is reduced. In these experiments the strength recovered
305 only partially, from approximately 0.7 MPa to approximately 1.3 MPa after a healing period of 12 hours. This



306 contrast between narrow-band and full-surface cracking highlights the important role of confinement and
307 compressive stresses in promoting healing.

308 Further evidence for the role of compressive stresses is provided by comparing the time required for thermal
309 equilibration with the time required for strength recovery. If healing occurred solely through the transformation of
310 the liquid-like layer into solid ice as the cracked region warmed, strength recovery would be expected to occur on
311 the same timescale as temperature recovery. In this case, the transformation is expected to occur almost
312 instantaneously, possibly within the same time frame as the Debye relaxation time. However, numerical calculations
313 show that the temperature of the thermally shocked ice recovers rapidly, within approximately 4 s, whereas the
314 recovery of flexural strength requires significantly longer times, typically 100–300 s (Fig. 2). This difference
315 suggests that additional time-dependent processes contribute to healing. The fact that strength recovery continues
316 well after thermal equilibration indicates that creep deformation and the development of contact between crack
317 surfaces play an important role.

318 In the previous study of narrow-band thermal cracking (Murdza et al., 2022a), the healing rate exhibited Arrhenius
319 behavior with an apparent activation energy comparable to that associated with surface diffusion on ice. That
320 observation led to the tentative interpretation that crack healing was primarily controlled by sintering via surface
321 diffusion. In light of the present results, however, the apparent activation energy likely reflects the combined
322 contribution of more than one process, including sintering at contacting crack surfaces and creep-assisted crack-tip
323 blunting. The presence of multiple processes operating simultaneously may therefore contribute to the uncertainty in
324 the activation-energy estimates obtained in the earlier analysis.

325 The increase in strength produced by compressive creep, resulting in a flexural strength of 1.56 ± 0.13 MPa, which
326 is statistically indistinguishable from the strength of pristine ice (1.67 ± 0.22 MPa; $p = 0.3$), can be understood in
327 terms of the geometry and deformation of asperities that protrude from opposing crack surfaces and interact at points
328 of contact. When two rough surfaces are brought into contact, the real contact area is typically much smaller than the
329 apparent area because contact occurs only at asperity tips. This concept, originally proposed by (Bowden and Tabor,
330 1950), implies that the actual contact area increases gradually as asperities deform. In the present case, creep
331 deformation under compressive stress increases the real contact area between opposing crack faces, thereby
332 promoting sintering and bond formation. The kinetics of strength recovery can be described by an Avrami-like
333 relationship (Avrami, 1939; Porter et al., 2009):

$$\frac{\sigma_r}{\sigma_0} = 1 - \exp(-kt^n), \quad (4)$$

334 where σ_0 is the initial strength of crack-free material, σ_r is the recovered strength, t is the healing time, and k and n
335 are kinetic parameters. Assuming that $\sigma_r/\sigma_0 = A_r/A_0$, where A_r and A_0 denote the real area and the apparent area



336 which is constant. Assuming that the recovered strength is proportional to the ratio of real to apparent contact area
337 and following the analysis of (Schulson et al., 2016), the recovered strength can be expressed as

$$\frac{\sigma_r}{\sigma_0} = \sigma_h B^{-1} t^n \exp(-nQ/RT), \quad (5)$$

338 where B is a material constant, σ_h is the compressive creep stress during healing, Q is an activation energy, R is the
339 gas constant and T is a temperature. Using parameter values reported by (Schulson et al., 2016), namely an
340 activation energy $Q = 50 \pm 6 \text{ kJ mol}^{-1}$, a material constant $B = 0.027 \text{ MPa s}^n$, and a stress exponent $n = 0.33$, and
341 taking $T = 263 \text{ K}$ and $R = 8.31 \text{ J mol}^{-1} \text{ K}^{-1}$, we obtain that for 1 hr of creep at the effective bending stress of $\sigma_h =$
342 0.5 MPa , $\sigma_r = 0.24 \text{ MPa}$.

343 This model predicts an increase in strength of approximately 0.24 MPa after one hour of creep at an effective
344 compressive stress of 0.5 MPa. In the present experiments, the observed increase in strength was $1.56 \text{ MPa} - 1.3$
345 $\text{MPa} = 0.26 \text{ MPa}$, which agrees well with the predicted value. Because the applied bending stress varies linearly
346 through the thickness of the specimen, the effective compressive stress acting on crack faces is approximately half
347 of the outer-fiber stress, which supports the assumption used in the calculation. This interpretation is consistent with
348 previous observations (Murdza et al., 2023), where strength recovery was enhanced when cyclic loading permitted
349 compressive contact between crack faces.

350 4.1 Creep-assisted blunting

351 Even when crack surfaces remain separated and cannot sinter, strength recovery can still occur through creep-
352 assisted blunting of crack tips. In the present experiments (v) this mechanism was examined by cyclically loading
353 thermally cracked specimens under non-reversed bending, ensuring that the cracked surface remained under tension
354 and that opposing crack faces did not come into contact. Under these conditions healing by sintering is suppressed.
355 Nevertheless, at $-10 \text{ }^\circ\text{C}$ the flexural strength recovered completely after approximately 10,000 seconds (Fig. 3),
356 whereas at $-28 \text{ }^\circ\text{C}$ only partial recovery was observed. This temperature dependence indicates that the process
357 responsible for recovery is thermally activated and consistent with creep-assisted crack-tip blunting.

358 In the competition between crack growth and crack blunting, blunting dominates as strength increases over time and
359 most likely tips of the cracks are getting blunted. Generally, according to the model proposed by (Renshaw and
360 Schulson, 2001), and crack blunting dominates crack growth when the size of the creep zone r_c ahead of the crack
361 tip exceeds the size of the elastic zone r_e , i.e. $r_c > r_e$. The size of the elastic zone can be estimated using Irwin's
362 approximation (Anderson, 2017; Irwin, 1957):

$$r_e = \frac{1}{6\pi} \left(\frac{K_I}{\sigma_e} \right)^2, \quad (6)$$



363 where K_I is the stress intensity. Assuming $\sigma_t = K_{Ic}/Y\sqrt{c}$, where K_{Ic} is the critical stress intensity factor (for both
364 freshwater and sea ice $K_{Ic} \approx 0.1 \text{ MPa}\sqrt{\text{m}}$ and depends on temperature, grain size, and loading rate; e.g., Schulson
365 and Duval., 2009; Rist et al., 2002; Weber and Nixon, 1996; Nixon and Schulson, 1988) and Y denotes a
366 geometrical factor, that we take to be of order unity, the elastic zone size becomes

$$r_e = \frac{c}{6\pi}. \quad (7)$$

367 For the cracks observed in the present experiments this yields $r_e \approx 0.1 \text{ mm}$.

368 When the ice is loaded slowly, creep occurs rapidly enough to prevent K_I from reaching K_{Ic} , therefore, promoting
369 macroscopically ductile behavior (Anderson, 2017; Broek, 1986; Schulson and Duval, 2009). The creep zone is
370 defined as the region within which creep strain exceeds elastic strain. The creep zone size can be estimated from the
371 Riedel–Rice model of creep zones around non-interacting cracks (Schulson and Duval, 2009):

$$r_c = \frac{K_I^2}{2\pi E^2} \left(\frac{(n+1)^2 E^n B t}{2n\zeta^{n-1}} \right)^{2/(n-1)} F, \quad (8)$$

372 where F denotes an angular function of order unity, ζ is a dimensionless factor.

373 Using material parameters for ice, this analysis yields $r_c = 5 \text{ mm}$. Since $r_c \gg r_e$, creep deformation occurs rapidly
374 enough to blunt the crack tip before the stress intensity reaches the critical value for crack propagation. Dislocation
375 activity ahead of the crack tip therefore absorbs energy during the loading and partial unloading portion of the load
376 cycle that would otherwise drive crack growth. A similar phenomenon of crack-tip blunting and arrest of fatigue
377 crack growth during non-reversed 4-point cyclic loading of freshwater ice was previously observed by (Weber and
378 Nixon, 1997).

379 Sea ice exhibits different behavior from freshwater ice. In both narrow-band and full-surface thermal shock
380 experiments the flexural strength of sea ice recovered completely within a short period. In addition, the thermally
381 induced cracks disappeared visually within a few seconds after the shock (a video recording of the rapid
382 disappearance of the cracks in the sea ice is provided in the Supporting Information of Murdza et. al (2022a)). We
383 attribute this rapid healing to the microstructural characteristics of sea ice, particularly its porous structure and the
384 presence of brine. Brine rapidly wets newly formed fracture surfaces and can refreeze quickly, facilitating rapid
385 healing. Furthermore, cracks propagating through sea ice frequently encounter pores and brine channels that act as
386 natural crack arresters, limiting crack length. The rapid disappearance of cracks and the quick recovery of strength
387 indicate a strong self-healing capability of sea ice associated with its microstructure. However, the present results
388 also suggest that healing kinetics may be strongly temperature dependent. At much lower temperatures, such as
389 those relevant to extraterrestrial icy environments, healing may occur significantly more slowly. For example, in our



390 earlier experiments at $-78\text{ }^{\circ}\text{C}$ the characteristic healing time of saline ice increased substantially compared with the
391 few seconds observed at $-10\text{ }^{\circ}\text{C}$. Whether thermal cracks in saline ice can heal rapidly under such extremely cold
392 conditions therefore remains an open question and warrants further investigation. However, because the number of
393 sea-ice experiments was limited and the associated uncertainties were relatively large, the apparent complete
394 recovery of strength should be interpreted cautiously.

395 The extent to which the present laboratory observations scale to natural ice covers remains an open question.
396 Processes such as sintering between contacting crack surfaces, liquid-like layer-assisted bonding, and creep-assisted
397 crack-tip blunting are expected to operate across scales because they are governed by material-level thermodynamic
398 and creep processes. However, their relative importance in natural environments may depend strongly on crack
399 geometry, confinement, thermal gradients, pore structure, brine transport, and loading history. In particular, the
400 compressive stresses generated during healing of narrow-band thermal cracks in laboratory specimens may be more
401 difficult to achieve in large-scale natural ice covers, where crack opening displacements and thermal gradients are
402 more heterogeneous. Similarly, the rapid healing observed in sea ice may depend on local brine connectivity and
403 pore structure, which vary substantially in natural environments. Nevertheless, the present experiments provide
404 insight into physical mechanisms that may contribute to strength recovery in thermally damaged ice.

405 If the behavior observed in laboratory-scale experiments reflects processes occurring at larger scales, the
406 implications for natural ice covers may differ between freshwater and sea ice. In freshwater ice, large regions
407 subjected to thermal cracking may not heal rapidly because the development of compressive stresses and
408 confinement may be limited. In contrast, sea ice may retain a greater capacity for rapid healing due to the presence
409 of brine within pores. However, the behavior of saline ice at extremely low temperatures remains uncertain and
410 requires further investigation.

411 **Conclusions**

412 Systematic experiments were conducted on the flexural strength of S2 columnar-grained freshwater, saline, and
413 first-year sea ice that were thermally cracked using liquid nitrogen and subsequently allowed either to heal at rest or
414 under cyclic loading at temperatures between $-78\text{ }^{\circ}\text{C}$ and $-3\text{ }^{\circ}\text{C}$. The results demonstrate that thermally induced
415 cracks do not necessarily lead to permanent weakening of ice. Instead, the flexural strength of cracked ice can
416 recover substantially, and in some cases almost completely, through two primary processes. The first involves
417 healing by contact between opposing crack surfaces, where sintering through surface diffusion and the presence of a
418 liquid-like layer promote the formation of bonds across the crack interface. This process is strongly enhanced by
419 compressive stresses that increase the real area of contact between crack faces. The second process involves creep-
420 assisted blunting of crack tips, a thermally activated mechanism that reduces stress concentration at the crack tip and
421 allows partial or complete recovery of strength even when crack faces remain separated.

422 The relative importance of these processes depends on temperature, loading conditions, and crack geometry. When
423 compressive stresses develop—either due to thermal expansion or externally applied loads—healing by contact



424 dominates. When crack surfaces remain separated, strength recovery can still occur through creep-assisted crack-tip
425 blunting, particularly at higher temperatures where creep processes are more active. In sea ice, healing occurs
426 particularly rapidly, likely due to the presence of brine and the porous microstructure, which facilitate rapid wetting
427 and refreezing of crack surfaces.

428 These findings suggest that thermally induced cracking may not permanently compromise the mechanical integrity
429 of natural ice covers, as healing processes can restore strength over timescales ranging from seconds to hours.
430 Understanding these processes is therefore important for predicting the mechanical behavior and stability of ice
431 covers in natural environments.

432 **Code and data availability**

433 The datasets supporting this study are publicly available through the Arctic Data Center repository:

- 434 • Murdza, A., Schulson, E., & Renshaw, C. (2024). *Study on creep-induced blunting of thermal cracks in*
435 *laboratory-produced freshwater ice and sea ice collected from the Beaufort Sea under cyclic loading and*
436 *creep, 2022–2024.* doi:10.18739/A2HT2GD4Z.
- 437 • Murdza, A., Schulson, E., & Renshaw, C. (2024). *Recovery of strength in locally versus globally thermally*
438 *cracked freshwater ice produced in the laboratory and sea ice collected in the Beaufort Sea, 2022–2024.*
439 doi:10.18739/A2NG4GT5C.
- 440 • Murdza, A., Schulson, E., & Renshaw, C. (2023). *Cyclic loading of freshwater ice produced in the*
441 *laboratory and sea ice collected in the Beaufort Sea with thermal microcracks, 2022–2023.*
442 doi:10.18739/A2HX15S3B.
- 443 • Murdza, A., Schulson, E., & Renshaw, C. (2022). *Healing of cracks in freshwater, saline and sea ice,*
444 *2020–2022.* doi:10.18739/A2HD7NT83.

445 **Author contributions**

446 AM, ES, and CR designed the experiments, and AM carried them out. AM prepared the manuscript with
447 contributions from all co-authors.

448 **Competing interests**

449 The authors declare that they have no conflict of interest.

450 **Acknowledgments**

451 We acknowledge the use of OpenAI's GPT-4 (Generative Pre-trained Transformer 4) via ChatGPT for assistance in
452 refining the written content.



453 **Financial support**

454 The authors acknowledge the National Science Foundation for financial support, grant no. FAIN 1947-107. We have
455 no financial conflicts of interest.

456 **References**

- 457 Anderson, T. L.: Fracture Mechanics: Fundamentals and Applications, Fourth Edition, Fracture Mechanics:
458 Fundamentals and Applications, Fourth Edition, 1–661, <https://doi.org/10.1201/9781315370293>, 2017.
- 459 Asakawa, H., Sazaki, G., Nagashima, K., Nakatsubo, S., and Furukawa, Y.: Two types of quasi-liquid layers on ice
460 crystals are formed kinetically, *Proc. Natl. Acad. Sci. U. S. A.*, 113, 1749–1753,
461 <https://doi.org/10.1073/pnas.1521607113>, 2016.
- 462 Avrami, M.: Kinetics of Phase Change. I General Theory, *J. Chem. Phys.*, 7, 1103–1112,
463 <https://doi.org/10.1063/1.1750380>, 1939.
- 464 Barrette, P. D. and Charlebois, L.: Winter roads and climate adaptation: Prospective solutions through R&D, in:
465 Conference of the Transportation Association of Canada, 2018.
- 466 Barrette, P. D. and Jordaan, I. J.: Healed cracks in iceberg ice, *Journal of Glaciology*, 48, 587–591,
467 <https://doi.org/10.3189/172756502781831179>, 2002.
- 468 Bazant, Z. P.: Large-scale thermal bending fracture of sea ice plates, *J. Geophys. Res. Oceans*, 97, 17739–17751,
469 <https://doi.org/10.1029/92JC00816>, 1992.
- 470 Bowden, F. P. and Tabor, D.: *The Friction and Lubrication of Solids*, Clarendon Press, Oxford, 1950.
- 471 Broek, D.: *Elementary engineering fracture mechanics*, 1st ed., Springer, Dordrecht, XIV, 469 pp.,
472 <https://doi.org/10.1007/978-94-009-4333-9>, 1986.
- 473 Bruce Martin, S. and Cott, P. A.: The under-ice soundscape in Great Slave Lake near the city of Yellowknife,
474 Northwest Territories, Canada, *J. Great Lakes Res.*, 42, 248–255, <https://doi.org/10.1016/J.JGLR.2015.09.012>,
475 2016.
- 476 Colbeck, S. C.: Theory of microfracture healing in ice, *Acta Metallurgica*, 34, 89–95, [https://doi.org/10.1016/0001-
477 6160\(86\)90235-X](https://doi.org/10.1016/0001-6160(86)90235-X), 1986.
- 478 Dash, J. G., Haiying Fu, and Wettlaufer, J. S.: The premelting of ice and its environmental consequences, *Reports on
479 Progress in Physics*, 58, 115, <https://doi.org/10.1088/0034-4885/58/1/003>, 1995.
- 480 Elbaum, M. and Schick, M.: Application of the theory of dispersion forces to the surface melting of ice, *Phys. Rev.
481 Lett.*, 66, 1713, <https://doi.org/10.1103/PhysRevLett.66.1713>, 1991.
- 482 Evans, R. J. and Untersteiner, N.: Thermal cracks in floating ice sheets, *J. Geophys. Res.*, 76, 694–703,
483 <https://doi.org/10.1029/JC076i003p00694>, 1971.
- 484 Faraday, M.: Note on Regelation, *Proc. Royal Soc. London*, 10, 440–450, 1860.
- 485 Filazzola, A., Imrit, M. A., Fleck, A., Woolway, R. I., and Sharma, S.: Declining lake ice in response to climate
486 change can impact spending for local communities, *PLoS One*, 19, e0299937,
487 <https://doi.org/10.1371/journal.pone.0299937>, 2024.



- 488 Fisher, D. A.: A process to make massive ice in the martian regolith using long-term diffusion and thermal cracking,
489 *Icarus*, 179, 387–397, <https://doi.org/10.1016/J.ICARUS.2005.07.024>, 2005.
- 490 Fransson, L. Å.: Do Cracks Reduce Thermal Ice Stresses?, in: *Ice-Structure Interaction*, 423–435,
491 https://doi.org/10.1007/978-3-642-84100-2_21, 1991.
- 492 Gold, L. W.: Formation of Cracks in Ice Plates by Thermal Shock, *Nature*, 192, 130–131,
493 <https://doi.org/10.1038/192130a0>, 1961.
- 494 Gold, L. W.: Crack formation in ice plates by thermal shock, *Can. J. Phys.*, 41, 1712–1728,
495 <https://doi.org/10.1139/P63-172>, 1963.
- 496 Golding, N., Snyder, S. A., Schulson, E. M., and Renshaw, C. E.: Plastic faulting in saltwater ice, *Journal of*
497 *Glaciology*, 60, 447–452, <https://doi.org/10.3189/2014JoG13J178>, 2014.
- 498 Goldreich, P. M. and Mitchell, J. L.: Elastic ice shells of synchronous moons: Implications for cracks on Europa and
499 non-synchronous rotation of Titan, *Icarus*, 209, 631–638, <https://doi.org/10.1016/J.ICARUS.2010.04.013>, 2010.
- 500 Hirata, N., Morishima, R., Ohtsuki, K., and Nakamura, A. M.: Disruption of Saturn’s ring particles by thermal
501 stress, *Icarus*, 378, 114919, <https://doi.org/10.1016/J.ICARUS.2022.114919>, 2022.
- 502 Iliescu, D., Murdza, A., Schulson, E. M., and Renshaw, C. E.: Strengthening ice through cyclic loading, *Journal of*
503 *Glaciology*, 63, 663–669, <https://doi.org/10.1017/jog.2017.32>, 2017.
- 504 Irwin, G. R.: Analysis of Stresses and Strains Near the End of a Crack Traversing a Plate, *J. Appl. Mech.*, 24, 361–
505 364, <https://doi.org/10.1115/1.4011547>, 1957.
- 506 Jones, B. M., Arp, C. D., Jorgenson, M. T., Hinkel, K. M., Schmutz, J. A., and Flint, P. L.: Increase in the rate and
507 uniformity of coastline erosion in Arctic Alaska, *Geophys. Res. Lett.*, 36, <https://doi.org/10.1029/2008GL036205>,
508 2009.
- 509 King, K., Fujisaki-Manome, A., Brant, C., Cohn, D., Peng, I., and Alofs, K.: Reconstructing Great Lakes air
510 temperature and ice dynamics data back to 1897, *Scientific Data* 2026 13:1, 13, 290–,
511 <https://doi.org/10.1038/s41597-026-06637-1>, 2026.
- 512 Kwok, R. and Rothrock, D. A.: Decline in Arctic sea ice thickness from submarine and ICESat records: 1958–2008,
513 *Geophys. Res. Lett.*, 36, 15501, <https://doi.org/10.1029/2009GL039035>, 2009.
- 514 Li, D. and Du, F.: Monitoring and evaluating the failure behavior of ice structure using the acoustic emission
515 technique, *Cold Reg. Sci. Technol.*, 129, 51–59, <https://doi.org/10.1016/j.coldregions.2016.06.003>, 2016.
- 516 Millerd, F.: The potential impact of climate change on Great Lakes international shipping, *Clim. Change*, 104, 629–
517 652, <https://doi.org/10.1007/S10584-010-9872-Z/METRICS>, 2011.
- 518 Milne, A. R.: Thermal tension cracking in sea ice: A source of underice noise, *J. Geophys. Res.*, 77, 2177–2192,
519 <https://doi.org/10.1029/JC077I012P02177>, 1972.
- 520 Murdza, A., Schulson, E. M., and Renshaw, C. E.: Strengthening of columnar-grained freshwater ice through cyclic
521 flexural loading, *Journal of Glaciology*, 66, 556–566, <https://doi.org/10.1017/jog.2020.31>, 2020.
- 522 Murdza, A., Schulson, E. M., and Renshaw, C. E.: Behavior of saline ice under cyclic flexural loading, *Cryosphere*,
523 15, 2415–2428, <https://doi.org/10.5194/tc-15-2415-2021>, 2021a.
- 524 Murdza, A., Marchenko, A., Schulson, E. M., and Renshaw, C. E.: Cyclic strengthening of lake ice, *Journal of*
525 *Glaciology*, 67, 182–185, <https://doi.org/10.1017/jog.2020.86>, 2021b.



- 526 Murdza, A., Polojärvi, A., Schulson, E. M., and Renshaw, C. E.: The flexural strength of bonded ice, *Cryosphere*,
527 15, 2957–2967, <https://doi.org/10.5194/tc-15-2957-2021>, 2021c.
- 528 Murdza, A., Schulson, E. M., Renshaw, C. E., and Polojärvi, A.: Rapid healing of thermal cracks in ice, *Geophys.*
529 *Res. Lett.*, 49, e2022GL099771, <https://doi.org/10.1029/2022gl099771>, 2022a.
- 530 Murdza, A., Schulson, E. M., and Renshaw, C. E.: Relaxation of Flexure-Induced Strengthening of Ice, *Geophys.*
531 *Res. Lett.*, 49, e2021GL096559, <https://doi.org/10.1029/2021GL096559>, 2022b.
- 532 Murdza, A., Schulson, E. M., and Renshaw, C. E.: Behavior Under Cyclic Loading of Freshwater Ice and Sea Ice
533 With Thermal Microcracks, *Geophys. Res. Lett.*, 50, e2023GL102889, <https://doi.org/10.1029/2023GL102889>,
534 2023.
- 535 Nguyen, N. N., Diger Berger, R., Kappl, M., and Rgen Butt, H.-J.: Clathrate Adhesion Induced by Quasi-Liquid
536 Layer, *J. Phys. Chem. C*, 125, <https://doi.org/10.1021/acs.jpcc.1c06997>, 2021.
- 537 Nixon, W. A. and Schulson, E. M.: The Fracture Toughness of Ice Over a Range of Grain Sizes, *Journal of Offshore*
538 *Mechanics and Arctic Engineering*, 110, 192–196, <https://doi.org/10.1115/1.3257050>, 1988.
- 539 Overeem, I., Anderson, R. S., Wobus, C. W., Clow, G. D., Urban, F. E., and Matell, N.: Sea ice loss enhances wave
540 action at the Arctic coast, *Geophys. Res. Lett.*, 38, 17503, <https://doi.org/10.1029/2011GL048681>, 2011.
- 541 Perovich, D. K., Richter-Menge, J. A., and Tucker, W. B.: Seasonal changes in Arctic sea-ice morphology, *Ann.*
542 *Glaciol.*, 33, 171–176, <https://doi.org/10.3189/172756401781818716>, 2001.
- 543 Petrenko, V. F. and Whitworth, R. W.: *Physics of Ice*, Oxford University Press,
544 <https://doi.org/10.1093/ACPROF:OSO/9780198518945.001.0001>, 1999.
- 545 Pistone, K., Eisenman, I., and Ramanathan, V.: Observational determination of albedo decrease caused by vanishing
546 Arctic sea ice, *Proc. Natl. Acad. Sci. U. S. A.*, 111, 3322–3326, <https://doi.org/10.1073/pnas.1318201111>, 2014.
- 547 Porter, D. A., Easterling, K. E., and Easterling, K. E.: *Phase Transformations in Metals and Alloys (Revised*
548 *Reprint)*, *Phase Transformations in Metals and Alloys (Revised Reprint)*, <https://doi.org/10.1201/9781439883570>,
549 2009.
- 550 Rampal, P., Weiss, J., and Marsan, D.: Positive trend in the mean speed and deformation rate of Arctic sea ice,
551 1979–2007, *J. Geophys. Res. Oceans*, 114, 5013, <https://doi.org/10.1029/2008JC005066>, 2009.
- 552 Renshaw, C. E. and Schulson, E. M.: Universal behaviour in compressive failure of brittle materials, *Nature* 2001
553 412:6850, 412, 897–900, <https://doi.org/10.1038/35091045>, 2001.
- 554 Rist, M. A., Sammonds, P. R., Oerter, H., and Doake, C. S. M.: Fracture of Antarctic shelf ice, *J. Geophys. Res.*
555 *Solid Earth*, 107, ECV 2-1, <https://doi.org/10.1029/2000jb000058>, 2002.
- 556 Schulson, E. M. and Duval, P.: *Creep and Fracture of Ice*, Cambridge University Press, Cambridge, 416 pp.,
557 <https://doi.org/10.1017/CBO9780511581397>, 2009.
- 558 Schulson, E. M. and Fortt, A. L.: Static strengthening of frictional surfaces of ice, *Acta Mater.*, 61, 1616–1623,
559 <https://doi.org/10.1016/J.ACTAMAT.2012.11.038>, 2013.
- 560 Schulson, E. M., Nodder, S. T., and Renshaw, C. E.: On the restoration of strength through stress-driven healing of
561 faults in ice, *Acta Mater.*, 117, 306–310, <https://doi.org/10.1016/J.ACTAMAT.2016.06.046>, 2016.
- 562 Schulson, E. M., Murdza, A., and Renshaw, C. E.: Mechanisms of Cyclic Strengthening and Recovery of
563 Polycrystalline Ice, in: *IUTAM Symposium on Physics and Mechanics of Sea Ice*, 3–8, 2022.



- 564 Smith, T. R. and Schulson, E. M.: The brittle compressive failure of fresh-water columnar ice under biaxial loading,
565 *Acta Metallurgica et Materialia*, 41, 153–163, [https://doi.org/10.1016/0956-7151\(93\)90347-U](https://doi.org/10.1016/0956-7151(93)90347-U), 1993.
- 566 Squire, V. A.: Of ocean waves and sea-ice revisited, *Cold Reg. Sci. Technol.*, 49, 110–133,
567 <https://doi.org/10.1016/j.coldregions.2007.04.007>, 2007.
- 568 Stewart, E. J., Howell, S. E. L., Draper, D., Yackel, J., and Tivy, A.: Sea Ice in Canada’s Arctic: Implications for
569 Cruise Tourism, *Arctic*, 60, 370–380, 2007.
- 570 Stroeve, J. C., Serreze, M. C., Holland, M. M., Kay, J. E., Malanik, J., and Barrett, A. P.: The Arctic’s rapidly
571 shrinking sea ice cover: a research synthesis, *Climatic Change* 2011 110:3, 110, 1005–1027,
572 <https://doi.org/10.1007/s10584-011-0101-1>, 2011.
- 573 Szabo, D. and Schneebeli, M.: Subsecond sintering of ice, *Appl. Phys. Lett.*, 90, 1–3,
574 <https://doi.org/10.1063/1.2721391>, 2007.
- 575 Thomson, J., Ackley, S., Girard-Ardhuin, F., Ardhuin, F., Babanin, A., Boutin, G., Brozena, J., Cheng, S., Collins,
576 C., Doble, M., Fairall, C., Guest, P., Gebhardt, C., Gemmrich, J., Graber, H. C., Holt, B., Lehner, S., Lund, B.,
577 Meylan, M. H., Maksym, T., Montiel, F., Perrie, W., Persson, O., Rainville, L., Erick Rogers, W., Shen, H., Shen,
578 H., Squire, V., Stammerjohn, S., Stopa, J., Smith, M. M., Sutherland, P., and Wadhams, P.: Overview of the Arctic
579 Sea State and Boundary Layer Physics Program, *J. Geophys. Res. Oceans*, 123, 8674–8687,
580 <https://doi.org/10.1002/2018JC013766>, 2018.
- 581 Timco, G. W. and O’Brien, S.: Flexural strength equation for sea ice, *Cold Reg. Sci. Technol.*, 22, 285–298,
582 [https://doi.org/10.1016/0165-232X\(94\)90006-X](https://doi.org/10.1016/0165-232X(94)90006-X), 1994.
- 583 Timco, G. W. and Weeks, W. F.: A review of the engineering properties of sea ice, *Cold Reg. Sci. Technol.*, 60,
584 107–129, <https://doi.org/10.1016/J.COLDREGIONS.2009.10.003>, 2010.
- 585 Weber, L. J. and Nixon, W. A.: Fracture Toughness of Freshwater Ice—Part I: Experimental Technique and Results,
586 *Journal of Offshore Mechanics and Arctic Engineering*, 118, 135, <https://doi.org/10.1115/1.2828822>, 1996.
- 587 Weber, L. J. and Nixon, W. A.: Fatigue of freshwater ice, *Cold Reg. Sci. Technol.*, 26, 153–164,
588 [https://doi.org/10.1016/S0165-232X\(97\)00014-1](https://doi.org/10.1016/S0165-232X(97)00014-1), 1997.
- 589 Yang, S., Yang, Y. Y., Zhang, J. Y., Zhang, Z. Y., Zhang, L., and Lin, X. C.: Laser-induced cracks in ice due to
590 temperature gradient and thermal stress, *Opt. Laser Technol.*, 102, 115–123,
591 <https://doi.org/10.1016/J.OPTLASTEC.2017.12.005>, 2018.
- 592 Zhang, R., Wang, H., Fu, Q., Rasch, P. J., and Wang, X.: Unraveling driving forces explaining significant reduction
593 in satellite-inferred Arctic surface albedo since the 1980s, *Proc. Natl. Acad. Sci. U. S. A.*, 116, 23947–23953,
594 <https://doi.org/10.1073/pnas.1915258116>, 2019.
- 595